Acta Crystallographica Section C
Crystal Structure Communications
ISSN 0108-2701

3-Deoxy-β-D-*ribo*-hexopyranose (3-deoxy-β-D-glucopyranose)

Wenhui Zhang, Bruce C. Noll and Anthony S. Serianni*

University of Notre Dame, Department of Chemistry and Biochemistry, 251 Nieuwland Science Hall, Notre Dame, IN 46556-5670, USA
Correspondence e-mail: aseriann@nd.edu

Received 18 May 2007
Accepted 6 August 2007
Online 1 September 2007

The β-pyranose form, (III), of 3-deoxy-D-*ribo*-hexose (3-deoxy-D-glucose), $C_6H_{12}O_5$, crystallizes from water at 298 K in a slightly distorted $^4C_1$ chair conformation. Structural analyses of (III), β-D-glucopyranose, (IV), and 2-deoxy-β-D-*arabino*-hexopyranose (2-deoxy-β-D-glucopyranose), (V), show significantly different C—O bond torsions involving the anomeric carbon, with the H—C—O—H torsion angle approaching an eclipsed conformation in (III) (−10.9°) compared with 32.8 and 32.5° in (IV) and (V), respectively. Ring carbon deoxygenation significantly affects the endo- and exocyclic C—C and C—O bond lengths throughout the pyranose ring, with longer bonds generally observed in the monodeoxygenated species (III) and (V) compared with (IV). These structural changes are attributed to differences in exocyclic C—O bond conformations and/or hydrogen-bonding patterns superimposed on the direct (intrinsic) effect of monodeoxygenation. The exocyclic hydroxymethyl conformation in (III) (*gt*) differs from that observed in (IV) and (V) (*gg*).

Comment

As part of ongoing NMR investigations of non-enzymic protein glycation (Voziyan *et al.*, 2003), ^{13}C-labeled 3-deoxy-D-*erythro*-hexos-2-ulose (3-deoxy-D-glucosone), (I), was prepared from ^{13}C isotopomers of 3-deoxy-D-*ribo*-hexose (3-deoxy-D-glucose), (II), using pyranose 2-oxidase (Freimund *et al.*, 1998). Compound (II) crystallizes from water in the β-pyranose form, (III) (Fig. 1), which is the predominant tautomeric form in aqueous solution (∼54%) (Pfeffer *et al.*, 1980).

Analysis of the Cremer–Pople puckering parameters (Cremer & Pople, 1975) for (III) and for the related aldohexoses β-D-glucopyranose, (IV) (Kouwijzer *et al.*, 1995), and 2-deoxy-β-D-*arabino*-hexose, (V) (Maluszynska *et al.*, 1981) (Table 1), shows that all three structures have slightly distorted $^4C_1$ chair forms ($q_3 >> q_2$). The degree of distortion varies with structure, with $\theta_{(IV)} > \theta_{(III)} > \theta_{(V)}$. The direction of distortion, embodied in the φ value, is similar for (IV) and (V), and both differ from (III). The φ values suggest a small tendency toward boat-like distortions for (III) and (V), and a twist-boat distortion for (IV) (Fig. 2), based on idealized φ values of 60° for (III), 330° for (IV) and 0° for (V).

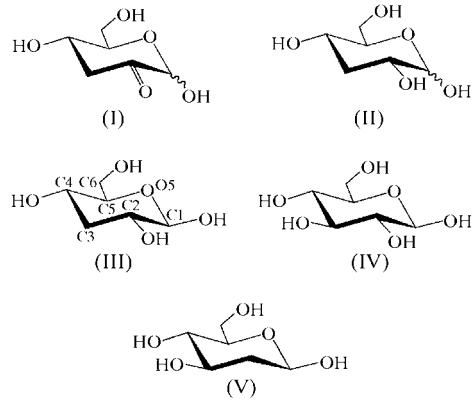

The structural parameters for compounds (III)–(V) are compared in Table 2. The C—C and C—O bond lengths vary considerably between the structures, with only the C5—C6 distance relatively unchanged. Of the three endocyclic C—C—C bond angles, the C1—C2—C3 angle changes the most (4.1°), and to approximately the same extent as the exocyclic C4—C5—C6 angle (3.9°). By comparison, the endocyclic C5—O5—C1 angle remains relatively unchanged between the three structures.

The endocyclic torsion angles (absolute values) range from 49.7 to 66.5°, indicative of the non-ideal character of the chair conformations. The C2—C1—O1—H bond torsions are similar in (IV) and (V) (∼153°) and are consistent with expectations based on the exoanomeric effect (Lemieux, 1971; Juaristi & Cuevas, 1995). Both are considerably larger than the corresponding torsion in (III) (∼111°). The latter torsion indicates a nearly eclipsed conformation for the H1—C1—O1—H torsion angle (−10.9°). Presumably, destabilization caused by eclipsing bonds is overcome by crystal packing forces to yield this otherwise higher-energy geometry.

Exocyclic hydroxymethyl conformation differs in compounds (III)–(V), with compound (III) favoring the *gt* conformation (C4 *anti* to O6), and compounds (IV) and (V) favoring the *gg* (H5 *anti* to O6) conformation. In solution, the *gg* and *gt* rotamers are considered more favored than the *tg*

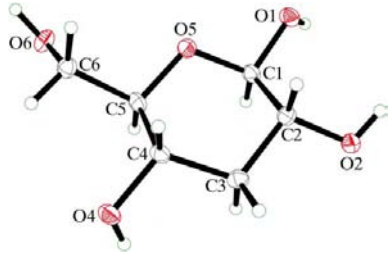

Figure 1
The molecular structure of (III), showing the atom-numbering scheme. Displacement ellipsoids are drawn at the 50% probability level and H atoms are shown as small spheres of arbitrary radii.

  DOI: 10.1107/S0108270107038553

rotamer (O5 *anti* to O6) in aldohexopyranosyl rings containing an equatorial C4—O4 bond (Thibaudeau *et al.*, 2004).

The presence of unquantifiable crystal packing forces complicates the interpretation of structural differences in compounds (III)–(V). Nevertheless, it is instructive to compare (III)–(V) by considering (IV) as the parent structure undergoing monodeoxygenation to give (V) or (III). The endocyclic bond lengths C3—C4, C5—C6 and C5—O5 are largely unchanged and the C1—C2, C2—C3 and C4—C5 bond lengths increase upon C3-deoxygenation. Only the C1—O5 bond length decreases. In contrast, bond lengths C5—C6, C5—O5 and C1—O5 remain largely unchanged and C1—C2, C4—C5 and possibly C2—C3 increase upon C2-deoxygenation. When endocyclic bond-length changes are observed upon monodeoxygenation at equatorial C—O bonds, they more often involve lengthening, *i.e.* they result in ring expansion/relaxation. The difference between the C1—O5 and C1—O1 bond lengths in (III) is considerably smaller (0.015 Å) than those observed in (IV) and (V) (0.037 and 0.045 Å, respectively), indicating different stereoelectronic properties at the anomeric sites.

The hydrogen bonding in (III) (Fig. 3) forms a dense three-dimensional network with no appreciable void space. The network is a 3^6-net made from four of eight possible connections (four donors and four acceptors). Two of the four connections, O4 and O6, are double bridges, acting as both donor and acceptor. Atom O6, acting as a donor, and atom O2, acting as an acceptor, complete the connections to form the two-dimensional corrugated sheet. The remaining connections, atom O6 as acceptor and atom O2 as donor, link the sheets into a stack. The hydrogen-bonding geometry is summarized in Table 3.

Different hydrogen-bonding patterns and/or exocyclic C—O torsions in compounds (III)–(V) may partly explain the bond-length changes observed upon monodeoxygenation. It is noteworthy that, apart from the different hydrogen-bonding properties of atoms O1 and H4O in compounds (IV) and (V), the hydrogen-bonding and C—O torsional behaviors are otherwise comparable, suggesting that the observed differences in bond lengths are caused mainly by deoxygenation effects. J_{CC} values in aqueous solution show $^1J_{C1,C2}$ to be larger in (IV) (46.0 Hz; King-Morris & Serianni, 1987) than in (V) (40.3 Hz; Bose *et al.*, 1998). A smaller $^1J_{CC}$ value would result from the longer C1—C2 bond in (V), superimposed on differences in substituent electronegativity effects at C2.

The differences in hydrogen-bonding patterns and C—O torsion angles are more pervasive in (III) and (IV) and could play a dominant role in determining some of the bond-length differences between these compounds. The latter possibility is supported by $^1J_{C1,C2}$ in (III) (46.9 Hz), which is 0.9 Hz larger than $^1J_{C1,C2}$ in (IV), despite the apparently larger C1—C2 distance observed in the crystal structure. Interestingly, $^1J_{C2,C3}$ is smaller in (III) (35.2 Hz) than in (IV) (38.8 Hz), consistent with the smaller C2—C3 distance in the latter. The significantly different C1—O1 torsion angles in (III) and (IV) (Table 2), and the altered hydrogen-bonding character of atoms O1 and O5, may be responsible for differences in their crystal structures near the anomeric C atom and elsewhere in the structure. The effects of C3-deoxygenation on the anomeric center are probably not long-range intrinsic effects induced solely by monodeoxygenation, but rather are mediated by extrinsic structural changes induced by crystal packing. Presumably, the C1—O1 torsion angles and other extrinsic characteristics in compounds (III) and (IV) are similar in aqueous solution, thus accounting for the comparable $^1J_{C1,C2}$ values observed in the solution state.

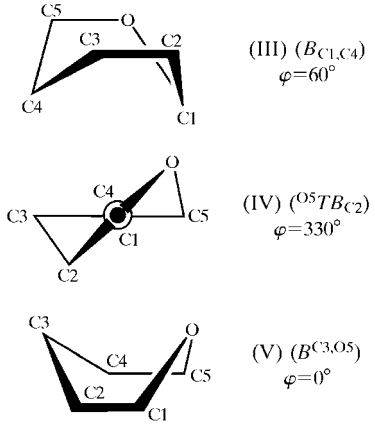

Figure 2
Ring distortions observed in compounds (III)–(V) based on Cremer–Pople parameters. *B* denotes the boat form and *TB* denotes the twist-boat form. The definition of φ is given in Cremer & Pople (1975).

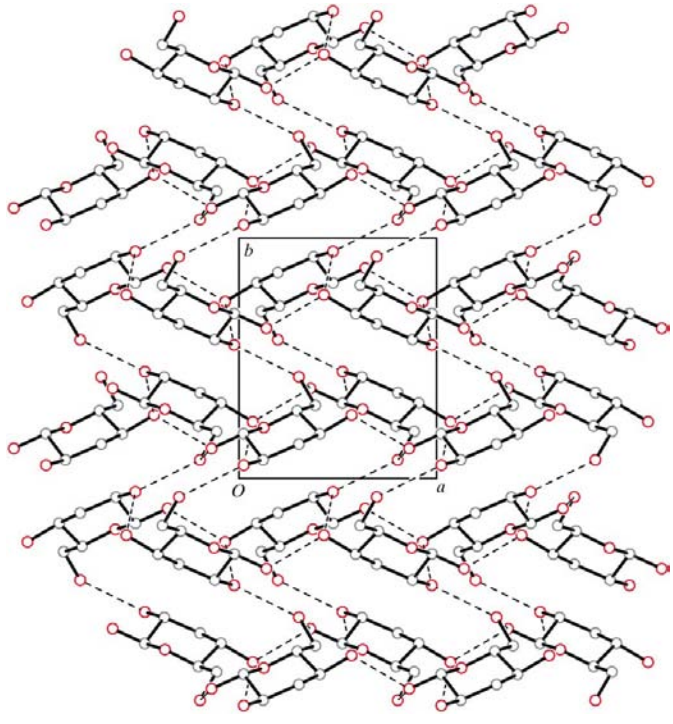

Figure 3
A packing diagram for (III), viewed down the *c* axis and parallel to the corrugated sheet structures formed by hydrogen bonding. Dashed lines indicate hydrogen bonding. H atoms have been omitted for clarity.

Experimental

1,2:5,6-Di-*O*-isopropylidene-α-D-glucofuranose (5.2 g, 20.0 mmol) was dissolved in tetrahydrofuran (100 ml), imidazole (30 mg) was added, and NaH (1.0 g, 40 mmol) was added batchwise. The reaction mixture was stirred for 1 h at room temperature under nitrogen. Carbon disulfide (6.0 ml, 100 mmol) was added and the mixture was stirred for 2 h. Methyl iodide (3.0 ml, 48 mmol) was added, and the mixture was stirred for an additional 1 h. The organic layer was washed with 1 *M* HCl, saturated $NaHCO_3$ and brine, and dried over anhydrous Na_2SO_4. After evaporation of the solvent, the residue was purified by silica-gel column chroatography (5:1 hexane–ethyl acetate) to afford 1,2:5,6-di-*O*-isopropylidene-3-*O*-(methylthio)thiocarbonyl-α-D-glucofuranose, (VI) (5.6 g, 80%).

Compound (VI) (3.5 g, 10 mmol) in toluene (60 ml) was added by dropping funnel (1 drop every 2 s) to tri-*n*-butyltin hydride (4.0 g) in toluene (50 ml) under nitrogen and under reflux. Refluxing was continued overnight and the solvent was removed with a rotary evaporator. Acetonitrile (40 ml) and hexane (40 ml) were added to the residue and the two-phase solution was stirred vigorously for 15 min. The lower acetonitrile layer was separated and the hexane phase washed with acetonitrile (15 ml). Extraction of the combined acetonitrile solutions was repeated twice. The combined acetonitrile phase was concentrated to give 1,2:5,6-di-*O*-isopropylidene-3-deoxy-α-D-*ribo*-hexofuranose, (VII) (2.1 g, 84%).

Compound (VII) (2.0 g, 8.2 mmol) was dissolved in 0.1% (*v*/*v*) aqueous H_2SO_4 (120 ml) and the reaction mixture was refluxed for 1 h in an oil bath. After cooling, the solution was treated with Dowex 1 × 8 (HCO_3^-) ion-exchange resin to adjust the pH to ∼7, the resin removed by filtration, and the solution concentrated at 303 K *in vacuo* to give 3-deoxy-D-*ribo*-hexose, (II) (1.1 g, 82%).

Compound (II) was dissolved in a minimal volume of distilled water and the solution was left at room temperature. Crystals of the title β-pyranose, (III), formed slowly and were harvested for structure determination.

Crystal data

$C_6H_{12}O_5$
M_r = 164.16
Orthorhombic, $P2_12_12_1$
a = 7.4534 (7) Å
b = 9.0663 (8) Å
c = 10.6966 (9) Å
V = 722.82 (11) Å^3
Z = 4
Cu $K\alpha$ radiation
μ = 1.14 mm^{-1}
T = 100 (2) K
0.21 × 0.19 × 0.19 mm

Data collection

Bruker SMART APEX CCD area-detector diffractometer
Absorption correction: multi-scan (*SADABS*; Sheldrick, 2004)
T_{min} = 0.795, T_{max} = 0.812
10176 measured reflections
1325 independent reflections
1311 reflections with $I > 2\sigma(I)$
R_{int} = 0.022

Refinement

$R[F^2 > 2\sigma(F^2)]$ = 0.026
$wR(F^2)$ = 0.069
S = 1.06
1325 reflections
104 parameters
H-atom parameters constrained
$\Delta\rho_{max}$ = 0.20 e Å^{-3}
$\Delta\rho_{min}$ = −0.20 e Å^{-3}
Absolute structure: Flack (1983), with 525 Friedel pairs
Flack parameter: 0.03 (19)

Table 1
Cremer–Pople puckering parameters for compounds (III)–(V).

Compound	θ (°)	φ (°)	Q (Å)	q_2 (Å)	q_3 (Å)
(III)	4.9	58.6	0.5736	0.0487	0.5715
(IV)	7.9	318.2	0.5802	0.0796	0.5747
(V)	3.9	350.5	0.5624	0.0379	0.5611

Table 2
Comparison of structural parameters for compounds (III)–(V).

	(III)†	(IV)‡	(V)§
C1—C2	1.5250 (18)	1.511 (4)	1.522 (5)
C2—C3	1.5216 (19)	1.513 (4)	1.522 (5)
C3—C4	1.5295 (18)	1.531 (4)	1.520 (5)
C4—C5	1.5329 (18)	1.519 (4)	1.530 (5)
C5—C6	1.5088 (18)	1.513 (4)	1.512 (5)
C1—O1	1.4005 (17)	1.394 (4)	1.386 (4)
C1—O5	1.4153 (16)	1.431 (3)	1.431 (4)
C2—O2	1.4227 (15)	1.429 (3)	
C3—O3		1.427 (3)	1.439 (5)
C4—O4	1.4325 (16)	1.422 (3)	1.427 (4)
C5—O5	1.4379 (16)	1.439 (3)	1.444 (4)
C6—O6	1.4289 (16)	1.424 (4)	1.433 (4)
C1—C2—C3	108.96 (10)	113.1 (2)	110.8 (3)
C2—C3—C4	110.76 (11)	109.8 (2)	110.9 (3)
C3—C4—C5	110.53 (11)	109.5 (2)	111.1 (3)
C4—C5—O5	110.62 (10)	108.3 (2)	109.3 (3)
C5—O5—C1	112.78 (10)	112.7 (2)¶	113.0 (3)
O5—C1—C2	109.76 (11)	109.3 (2)	110.5 (3)
C4—C5—C6	111.06 (11)	115.0 (2)	113.6 (3)
C1—C2—C3—C4	−54.39 (14)	−49.7 (3)	−51.3 (4)
C1—O5—C5—C4	60.09 (13)	66.5 (3)	61.3 (4)
C2—C3—C4—C5	51.35 (14)	52.6 (3)	51.9 (4)
C2—C1—O5—C5	−63.83 (13)	−61.9 (3)	−61.5 (4)
C3—C4—C5—O5	−52.64 (14)	−60.5 (3)	−55.6 (4)
C3—C2—C1—O5	59.82 (13)	53.2 (3)	55.2 (4)
C2—C1—O1—H	111	153	153
O5—C1—O1—H	−130	−90	−87 (3)
O5—C5—C6—O6	74.22 (13) (*gt*)	−60.4 (3) (*gg*)	−64.8 (4) (*gg*)

† 3-Deoxy-β-D-glucopyranose (this work). ‡ β-D-Glucopyranose (Kouwijzer *et al.*, 1995). § 2-Deoxy-β-D-glucopyranose (Maluszynska *et al.*, 1981). ¶ Taken from Chu & Jeffrey (1968).

Table 3
Hydrogen-bond geometry (Å, °).

D—H···A	D—H	H···A	D···A	D—H···A
O1—H1O···O4^{i}	0.84	1.81	2.6381 (13)	169
O2—H2O···O6^{ii}	0.84	1.92	2.7222 (14)	159
O4—H4O···O2^{iii}	0.84	1.87	2.7090 (14)	176
O6—H6O···O1^{iv}	0.84	1.94	2.7742 (14)	175

Symmetry codes: (i) $x+1, y, z$; (ii) $-x+1, y+\frac{1}{2}, -z+\frac{3}{2}$; (iii) $x-\frac{1}{2}, -y+\frac{3}{2}, -z+2$; (iv) $x-\frac{1}{2}, -y+\frac{3}{2}, -z+1$.

H atoms were positioned geometrically and treated as riding, with O—H = 0.84 Å and C—H = 0.99–1.00 Å, and with U_{iso}(H) = 1.2U_{eq}(C) or 1.5U_{eq}(O).

Data collection: *APEX2* (Bruker, 2006); cell refinement: *APEX2* and *SAINT* (Bruker, 2006); data reduction: *SAINT* and *XPREP* (Sheldrick, 2005); program(s) used to solve structure: *XL* (Sheldrick, 2001); program(s) used to refine structure: *XS* (Sheldrick, 2001); molecular graphics: *XP* (Sheldrick, 1998); software used to prepare material for publication: *XCIF* (Sheldrick, 2001) and *enCIFer* (Allen *et al.*, 2004).

The authors thank Professor Kenneth W. Henderson for assistance in describing the hydrogen-bonding network. This work was supported by the National Institute of Diabetes and Digestive and Kidney Disease, research grant No. DK065138.

Supplementary data for this paper are available from the IUCr electronic archives (Reference: SF3042). Services for accessing these data are described at the back of the journal.

References

Allen, F. H., Johnson, O., Shields, G. P., Smith, B. R. & Towler, M. (2004). *J. Appl. Cryst.* **37**, 335–338.

Bose, B., Zhao, S., Stenutz, R., Cloran, F., Bondo, P. B., Bondo, G., Hertz, B., Carmichael, I. & Serianni, A. S. (1998). *J. Am. Chem. Soc.* **120**, 11158–11173.

Bruker (2006). *APEX2* and *SAINT*. Bruker–Nonius AXS Inc., Madison, Wisconsin, USA.

Chu, S. S. C. & Jeffrey, G. A. (1968). *Acta Cryst.* B**24**, 830–838.

Cremer, D. & Pople, J. A. (1975). *J. Am. Chem. Soc.* **97**, 1354–1358.

Flack, H. D. (1983). *Acta Cryst.* A**39**, 876–881.

Freimund, S., Huwig, A., Giffhorn, F. & Köpper, S. (1998). *Chem. Eur. J.* **4**, 2442–2455.

Juaristi, E. & Cuevas, G. (1995). *The Anomeric Effect*. Boca Raton: CRC Press.

King-Morris, M. J. & Serianni, A. S. (1987). *J. Am. Chem. Soc.* **109**, 3501–3508.

Kouwijzer, M. L. C. E., van Eijck, B. P., Kooijman, H. & Kroon, J. (1995). *Acta Cryst.* B**51**, 209–220.

Lemieux, R. U. (1971). *Pure Appl. Chem.* **25**, 527–548.

Maluszynska, H., Ruble, J. R. & Jeffrey, G. A. (1981). *Carbohydr. Res.* **97**, 199–204.

Pfeffer, P. E., Parrish, F. W. & Unruh, J. (1980). *Carbohydr. Res.* **84**, 13–23.

Sheldrick, G. M. (1998). *XP*. Bruker AXS Inc., Madison, Wisconsin, USA.

Sheldrick, G. M. (2001). *XCIF*, *XL* and *XS*. Bruker–Nonius AXS Inc., Madison, Wisconsin, USA.

Sheldrick, G. M. (2004). *SADABS*. University of Göttingen, Germany.

Sheldrick, G. M. (2005). *XPREP*. Bruker–Nonius AXS Inc., Madison, Wisconsin, USA.

Thibaudeau, C., Stenutz, R., Hertz, B., Klepach, T., Zhao, S., Wu, Q., Carmichael, I. & Serianni, A. S. (2004). *J. Am. Chem. Soc.* **126**, 15668–15685.

Voziyan, P. A., Khalifah, R. G., Thibaudeau, C., Yildiz, A., Jacob, J., Serianni, A. S. & Hudson, B. G. (2003). *J. Biol. Chem.* **278**, 46616–46624.